Corticothalamic synchronization leads to *c-fos* expression in the auditory thalamus

Yi Ping Guo*, Xia Sun*†, Chuan Li*, Ning Qian Wang*, Ying-Shing Chan†, and Jufang He*‡

*Department of Rehabilitation Sciences, Hong Kong Polytechnic University, Hung Hom, Kowloon, Hong Kong, China; and †Department of Physiology and Research Centre of Heart, Brain, Hormone, and Healthy Aging, LKS Faculty of Medicine, University of Hong Kong, Sassoon Road, Hong Kong, China

Edited by Edward G. Jones, University of California, Davis, CA, and approved May 17, 2007 (received for review February 12, 2007)

In this study, we investigated the relationship between *c-fos* expression in the auditory thalamus and corticofugal activation. The contribution of neurotransmitters and related receptors, the involvement of thalamic reticular nucleus (TRN), and the role of neuronal firing patterns in this process were also examined. The principal nuclei of the medial geniculate body (MGB) showed *c-fos* expression when the auditory cortex (AC) was activated by direct injection of bicuculline methobromide. However, no expression was detectable with acoustic stimuli alone. This indicated that *c-fos* expression in the principal nuclei of the MGB was triggered by the corticofugal projection. *c-fos* expression could be elicited in the MGB by direct injection of glutamate. Direct administration of acetylcholine, alternatively, had no effect. Bicuculline methobromide injection in the AC also triggered synchronized oscillatory activities sequentially in the AC and MGB. Cortically induced *c-fos* expression in the MGB was not mediated by a pathway involving the TRN because it remained intact after a TRN lesion with kainic acid. The present results also conclude that *c-fos* expression is not simply associated with firing rate, but also with neuronal firing pattern. Burst firings that are synchronized with the cortical oscillations are proposed to lead to *c-fos* expression in the principal nuclei of the MGB.

activity marker | cortical activation | Fos | glutamate receptor | medial geniculate body

The thalamus relays sensory information to the cortex and, in return, receives massive feedback projections from the cortex (1–4). Corticothalamic projections are suggested to provide a gain-control mechanism on the transmission of sensory information (5–7) and to play an important role in the generation of neural oscillations (8–10). The thalamic reticular nucleus (TRN) is thought to be involved in the corticothalamic process and the genesis of the oscillations (1, 3). In the auditory system, high-frequency oscillation can be generated in the cortex, evoked by acoustic stimuli, and modulated by the thalamic stimulation (11). A slow oscillation of <1 Hz and a spindle-like oscillation of 5–10 Hz have also been described recently in the auditory thalamus (12).

Neuronal expression of Fos protein after novel physiological input constitutes a useful marker for polysynaptic activation, allowing subpopulations of neurons in specific neuronal circuits to be identified (13, 14). Fos-immunoreactivity has also been used to identify functionally activated neurons in the ascending auditory system (15–19). *c-fos*, however, did not express in the ventral and dorsal divisions of the MGB when the subject was exposed to acoustic stimulation in isolation (18, 19).

In an attempt to study the contribution of the corticofugal projection to thalamic neurons in the ascending auditory circuitry using *c-fos* as an activity marker, we found heavy Fos labeling in the MGB after the auditory cortex was activated by injecting bicuculline methobromide (BIM, a $GABA_A$ receptor antagonist). In the present study, we investigated the relationship between *c-fos* expression in the auditory thalamus and corticofugal activation, the contribution of several neurotransmitters and related receptors, the involvement of TRN and the role of neuronal firing patterns in this process.

Results

***c-fos* Expression in the MGB Is Triggered by Cortical Activation.** Acoustic stimuli elicited no *c-fos* expression in the ventral division (MGv) and dorsal division (MGd) of MGB of anesthetized rats (Fig. 1*A*). Various acoustic stimuli, including pure tones of different frequencies and noise bursts of repetitive rates of 1–3 Hz, were applied to the rats for 1–4 h. Although *c-fos* expression was found in the cochlear nucleus, superior olivary complex (data not shown), and inferior colliculus [supporting information (SI) Fig. 6], only a few Fos-positive neurons were detected in the MGB, with no labeling in the MGv and only sporadically scattered labeling in the MGm (Fig. 1*A*). By contrast, the MGv and MGd showed extensive *c-fos* expression after cortical BIM injection (Fig. 1*B*). Both MGv and MGd were most strongly labeled, extending along the rostrocaudal dimension. Control saline injections did not result in cortical and thalamic *c-fos* expression (data not shown). Furthermore, *c-fos* expression after unilateral cortical BIM injection was restricted to the ipsilateral MGB and cortex (Fig. 1*B*).

***c-fos* Expression Is Elicited by Glutamate but Not by Acetylcholine.** To understand the dependence of *c-fos* expression on neurotransmitters that are related to descending and ascending projections, we injected glutamate and acetylcholine in the MGB. Direct injection of glutamate in the auditory thalamus elicited *c-fos* expression in thalamocortical projection neurons (Fig. 1*C Left*), whereas injection of acetylcholine did not evoke *c-fos* expression in the MGv (Fig. 1*C Right*). The induction of *c-fos* expression in the MGB by glutamate injection depended on the level of anesthesia. Rats that were not administered further anesthesia after the glutamate injection procedure showed *c-fos* expression as in Fig. 1*C*, whereas those that were continuously supplemented with anesthesia during their survival period showed no *c-fos* expression in the MGB (data not shown).

We next examined the glutamate receptors involved in *c-fos* expression in the MGB. After BIM injection in the auditory cortex (AC), the MGB of all rats showed heavy labeling of Fos-positive neurons (Fig. 2*A*). Antagonists of all three types of glutamate receptors, AP-V (for NMDA receptor), CNQX (for AMPA receptor), and LY367385 (for metabotropic glutamate receptor, mGluR1α), showed a strong suppressive effect on the *c-fos* expression elicited by corticofugal activation (BIM injection in the AC) (Fig. 2 *B–D*). The diffusions of injections were demarcated by mixed

Author contributions: X.S., C.L., and N.Q.W. contributed equally to this work; Y.P.G. and J.H. designed research; Y.P.G., X.S., C.L., and N.Q.W. performed research; Y.-S.C. contributed new reagents/analytic tools; Y.P.G., X.S., Y.-S.C., and J.H. analyzed data; and Y.P.G., Y.-S.C., and J.H. wrote the paper.

The authors declare no conflict of interest.

This article is a PNAS Direct Submission.

Abbreviations: MGB, medial geniculate body; BIM, bicuculline methobromide; AC, auditory cortex; TRN, thalamic reticular nucleus; KA, kainic Acid; MGv, ventral division of medial geniculate body; MGd, dorsal division of MGB.

‡To whom correspondence should be addressed. E-mail: rsjufang@polyu.edu.hk.

This article contains supporting information online at www.pnas.org/cgi/content/full/0701302104/DC1.

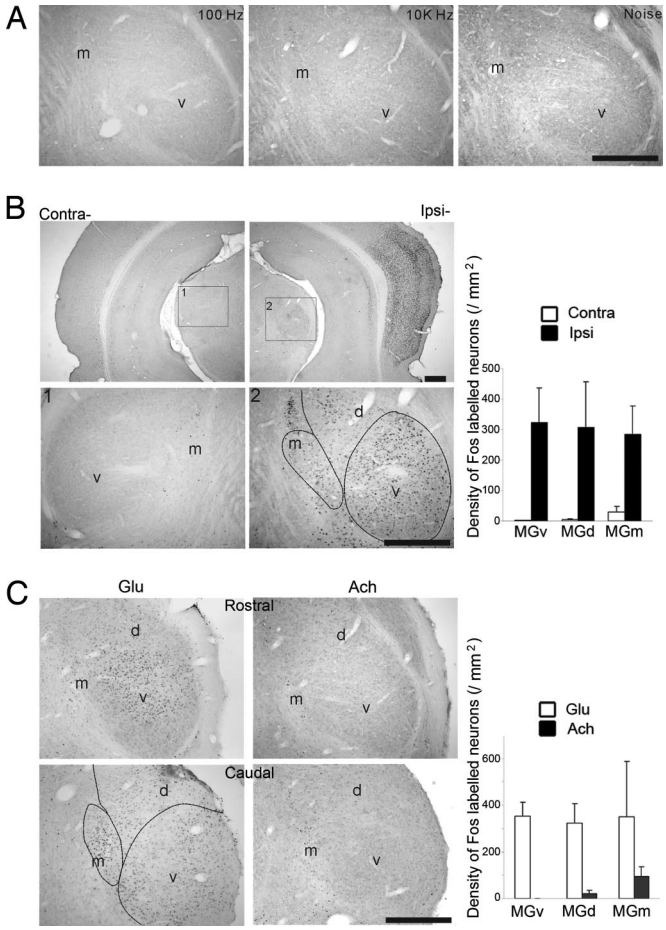

Fig. 1. *c-fos* expression in the AC and MGB. (*A*) Acoustic stimuli evoked no labeling in the MGB. Stimuli included pure tones (100 Hz and 10 kHz) and noise bursts. (*B*) Photomicrographs of the bilateral cortex and MGB at low-power magnification (*Upper*) and that of the MGB at high-power magnification (*Lower*) after BIM was injected into the ipsilateral AC. (*C*) *c-fos* expression after injection of glutamate (*Left*, Glu → MGB) or acetylcholine (*Right*, Ach → MGB) in the MGB. Upper and lower images show the MGB at two different caudorostral levels. Histogram on the right shows the densities of Fos-positive neurons in the different MGB divisions. Significant differences ($P < 0.01$) were found in both *B* ($n = 6$ rats) and *C* ($n = 3$ for each). v, ventral division, MGv; d, dorsal division, MGd; m, medial division, MGm. This convention applies to all figures. (Scale bars, 400 μm.)

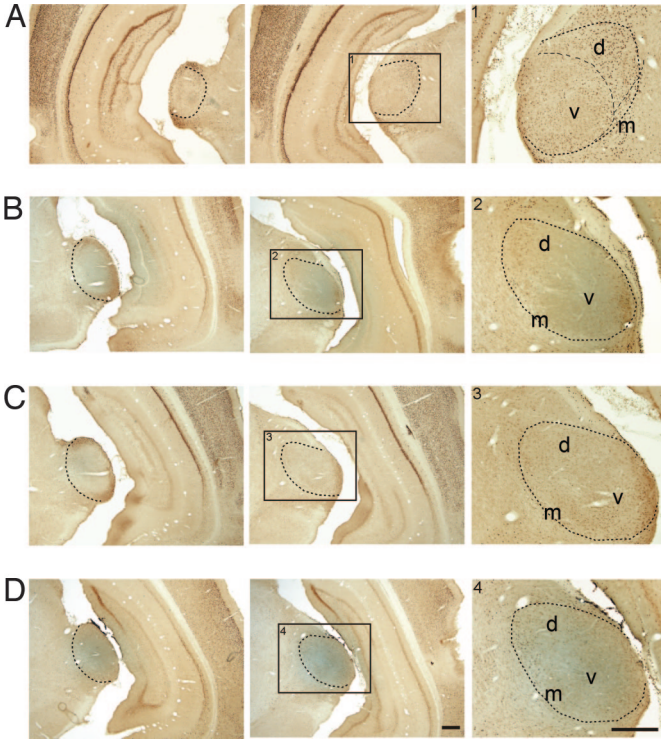

Fig. 2. Corticofugally triggered *c-fos* expression in the MGB was suppressed by glutamate receptor antagonists. The rats were injected with BIM in the AC and with saline (*A*), or with antagonists of NMDA receptor, AP-V (*B*), antagonist of AMPA receptor, CNQX (*C*), and antagonist of metabotropic glutamate receptor, LY367385 (*D*) in the MGB. The left two columns show two coronal sections at different rostrocaudal levels. Regions marked with rectangles, 1, 2, 3, and 4, in the center column are shown (*Right*) with higher magnification. The principle nuclei of MGB are included within the dotted lines. The blue color illustrates the diffusions of injections. (Scale bars, 400 μm.)

Pontamine skyblue (1%). The injection of CNQX, shown in Fig. 2*C*, was locally restricted to the caudal MGB so that the suppression of *c-fos* expression in the middle and rostral MGB was relatively weaker than that produced by the injection of NMDA and mGluR1α receptor antagonists that spread more rostrally (Fig. 2 *B* and *D*). All three antagonists of glutamate receptors had an effect in eliminating *c-fos* expression in the MGv.

Activation of the Auditory Cortex Triggers Thalamocortical Synchronization. To examine the physiological relationship between the cortex and the thalamus, we monitored neural activities in the thalamus and cortex through multichannel extracellular recordings. Fig. 3*A* shows multichannel extracellular recordings from the MGB (Th1–Th4) and the auditory cortex (Cx) before, during, and after BIM injection in the AC. The recording sites Th1–Th3 and Cx responded to acoustic stimulus (Fig. 3*B*). Spontaneous neuronal activities were observed in all recordings in the MGB and the AC. These activities were not well synchronized before BIM injection in the cortex (Fig. 3*A Left*). The auditory cortex started a rhythmic activity during the course of BIM injection into the AC (Fig. 3*A Middle*). An increased spontaneous activity and rhythmic burst firings then occurred in the all recording sites, and a corticothalamic synchrony developed 6.8 ± 3.9 min ($n = 13$) after cortical BIM injection. Fig. 3*A Right* shows neuronal activities of the thalamus and cortex 12 min after BIM injection. In this case, the cortex and thalamus developed a highly synchronized activity with a rhythm of 2.8 Hz and a lag time of <50 ms. From the expanded traces (Fig. 3*A Right*), it was found that bursts in the cortex occurred before those of the thalamus. The cross-correlograms revealed that there were no obvious correlations between the cortical and thalamic events before BIM injection. Rhythmic activity and the synchrony between the MGB and AC started during BIM injection (Fig. 3*A Center*) and fully developed after BIM injection (Fig. 3*A Right*). This was confirmed in all subjects with a rhythmic oscillation of 0.3–3 Hz (mainly 1–3 Hz) after BIM injection in the AC.

Firing Patterns and *c-fos* Expression. Because *c-fos* is considered as a marker of incremental activity (14, 20), the correlation between *c-fos* expression and neuronal activity was examined. Eighteen single units, 8 recorded before and 10 after BIM injection to the AC, were isolated from two BIM → AC rats. Eighteen other single units, eight recorded before and ten during the presentation of acoustic stimulus (AS), were isolated from two AS rats. Another eight single units, recorded at ≈10 min after the injection of kainic acid (KA) to the MGB, were isolated from two KA → MGB rats. KA, known to selectively destroy cells in the injected region but not axons coursing through the area, was used here to activate MGB neurons for a short period of 1 h.

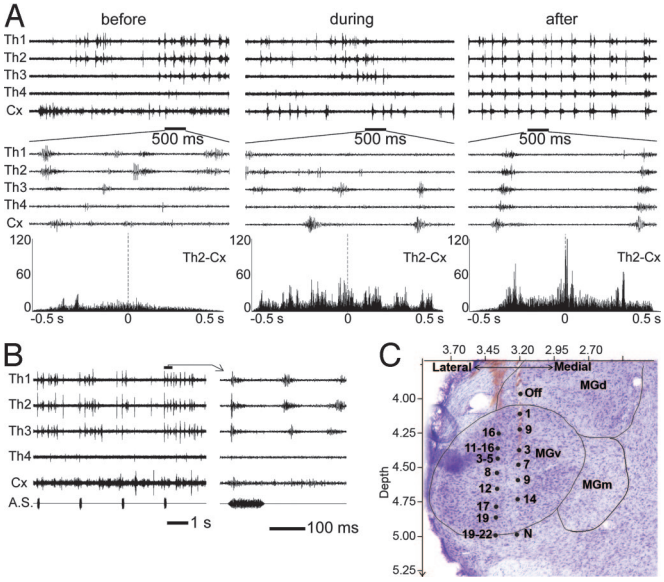

Fig. 3. Multichannel recordings of neuronal activities in the thalamus and cortex. (*A*) Recordings from the MGB (Th1–4, 5.9, 5.4, 5.0, and 4.5 mm caudal to Bregma, 4,500-μm depth) and the auditory cortex (Cx, 0.8 mm in depth) measured spontaneous neuronal activities before, during, and after BIM injection in the AC. (*Top*) The neuronal activities in a long time scale. (*Middle*) Neuronal activities in short time scale. (*Bottom*) The cross-correlograms between the recordings of Th2 and the Cx. (*B*) Neuronal responses to repeated noise-burst stimuli in the same recording sites as in *A*. Recordings were carried out before the BIM injection to confirm MGB and AC. The marked episode (*Left*) is expanded (*Right*). (*C*) Physiological mapping superimposed on Nissl staining. The plane was at a rostrocaudal coordinate (RC) of 5.5 mm. Vertical coordinate indicates the depth from the cortical surface. Horizontal coordinate indicates the mediolateral distance from midline (in millimeters). Numbers beside the black circles indicate the characteristic frequency (CF, in kHz).

Fig. 4*A* illustrates the raster displays of three single neurons, respectively from the three paradigms listed above. Fig. 4*A Left* shows the spontaneous neuronal activities before (control) and after BIM injection. Fig. 4*A Center* shows spontaneous activities before (control) and during the delivery of repeated acoustic stimuli. Fig. 4*A Right* illustrates spontaneous activities after KA injection. It was obvious that the firing rates after BIM or KA injection and during acoustic stimulus were significantly higher than those under control conditions (Fig. 4*A*). The spontaneous firing before KA injection can be assumed to be similar to the spontaneous firings shown in the other controls (Fig. 4*A Upper*).

The mean firing rates over 20 s were calculated for neurons in each of the three conditions and were summarized in Fig. 4*B*. The means of all controls were similar (BIM $\rightarrow$ AC, 1.10 $\pm$ 0.62 spikes per second; AS, 1.57 $\pm$ 0.67; $P > 0.05$, ANOVA). The firing rates increased significantly in all experimental conditions compared with controls (BIM $\rightarrow$ AC, 4.77 $\pm$ 1.87 spikes per second; AS, 5.20 $\pm$ 1.42; $P < 0.05$, *t* test; KA, 4.79 $\pm$ 0.98; Fig. *4B*). Although the firing rates of neurons in different experimental conditions were not significantly different ($P > 0.05$, ANOVA), their temporal patterns (Fig. 4*A Lower*) were different: BIM $\rightarrow$ AC showed spontaneous burst-like firings synchronized with AC, whereas AS showed response fixed to auditory stimuli, and KA showed single spikes.

An example of *c-fos* expression in the MGB for each of above three paradigms is shown in Fig. 4*C*. In both groups of AS and KA $\rightarrow$ MGB, no *c-fos* expression was elicited in the MGv. *c-fos* expression was detected only in the MGv of BIM $\rightarrow$ AC rats. Considering that all three paradigms had similar firing rates or similar increments in firing rate, the result that only BIM $\rightarrow$ AC rats had *c-fos* expression in the MGB could lead to the conclusion that *c-fos* expression in the MGv was not simply a reflection of neuronal activity or the increment of neuronal activity.

Corticothalamic Synchrony and Thalamic *c-fos* Expression Is Not Altered by TRN. We understand that most thalamocortical oscillations are engaged with the TRN. Strong TRN inhibition causes a prolonged hyperpolarization of MGB neurons, which may lead to low-threshold calcium spikes or spike bursts (8–10, 21). It is, however, unknown whether the corticothalamic synchrony caused by cortical BIM injection is mediated by TRN. We observed a heavy labeling of neurons in the auditory sector of TRN after activation of the AC with BIM (Fig. 5*A Upper*). This prompted us to examine whether *c-fos* expression in MGv neurons was evoked or affected by inhibitory inputs from TRN.

The rats were injected with BIM in the AC at 2–7 days after a TRN lesion in the auditory sector. The TRN lesion in the auditory sector was confirmed with Nissl staining, comparing the left (no lesion) and right (lesion) thalamus from the same section (Fig. 5*C*). No Fos-positive neurons could be detected in the auditory sector of the TRN after lesion (Fig. 5*A Lower*), also confirming that the TRN neurons were damaged.

c-fos expression in the MGv after TRN lesion (Fig. 5*B Left*) was similar to *c-fos* expression without TRN lesion (shown in Figs. 1 and 5*E*), indicating that the indirect pathway of AC–TRN–MGB exerted no determining effect on *c-fos* expression in the MGB. A parallel experiment, in which rats received GABA injection to the MGB and BIM injection to the AC (Fig. 5*B Right*), again had no significantly positive effect on *c-fos* expression in the MGB. Both experiments demonstrated that the TRN is unlikely to play a role in corticofugally induced *c-fos* expression in the MGB.

Fig. 5*D* shows the effect of TRN lesion on thalamic and cortical neuronal activities after the cortex was activated with BIM. Electrophysiological recordings show that TRN lesion did not alter the frequency or duration of the synchrony between the AC and MGB. This indicates that the direct corticofugal pathway prevailed over the indirect pathway in producing synchrony in the MGB.

Discussion

***c-fos* Expression in the Auditory Pathway.** Physiological experiments have shown that the MGB neurons respond to sound stimuli even under the anesthetized condition. In this study, we could not elicit *c-fos* expression in the MGv with an acoustic stimulus, repeated electrical stimulation of the inferior colliculus (data not shown), or direct KA injection in the MGB. These results demonstrate that the corticofugal projection was crucial to elicit *c-fos* expression in most subnuclei of the MGB. Another implication of these results is that the descending cortical projection in the thalamus is much more physiologically powerful than the ascending projection from the inferior colliculus.

Studies have shown that cochlear nuclear neurons and inferior colliculus neurons express *c-fos* upon activation by acoustic stimulus. MGv neurons, alternatively, showed no *c-fos* expression in response to acoustic stimuli (refs. 17–19 and Fig. 1*A*). Only one other experiment has shown *c-fos* expression in the MGv (22). In that experiment, *c-fos* expression was elicited in the MGB after the subject acquired a visually cued conditioned fear. The authors concluded that the *c-fos* expression was elicited by a newly established pathway from the retina directly to the MGB. This was a highly speculative explanation, because there was no anatomical proof for the formation of such a circuit, and it was unclear whether the new circuit could be formed within 14 weeks. Additionally, there was no report that the ascending pathway could activate *c-fos* expression in the MGv. It is more likely that the fear conditioning caused an activation of the corticothalamic projection, which in turn activated the MGB by a process similar to that observed in the present study.

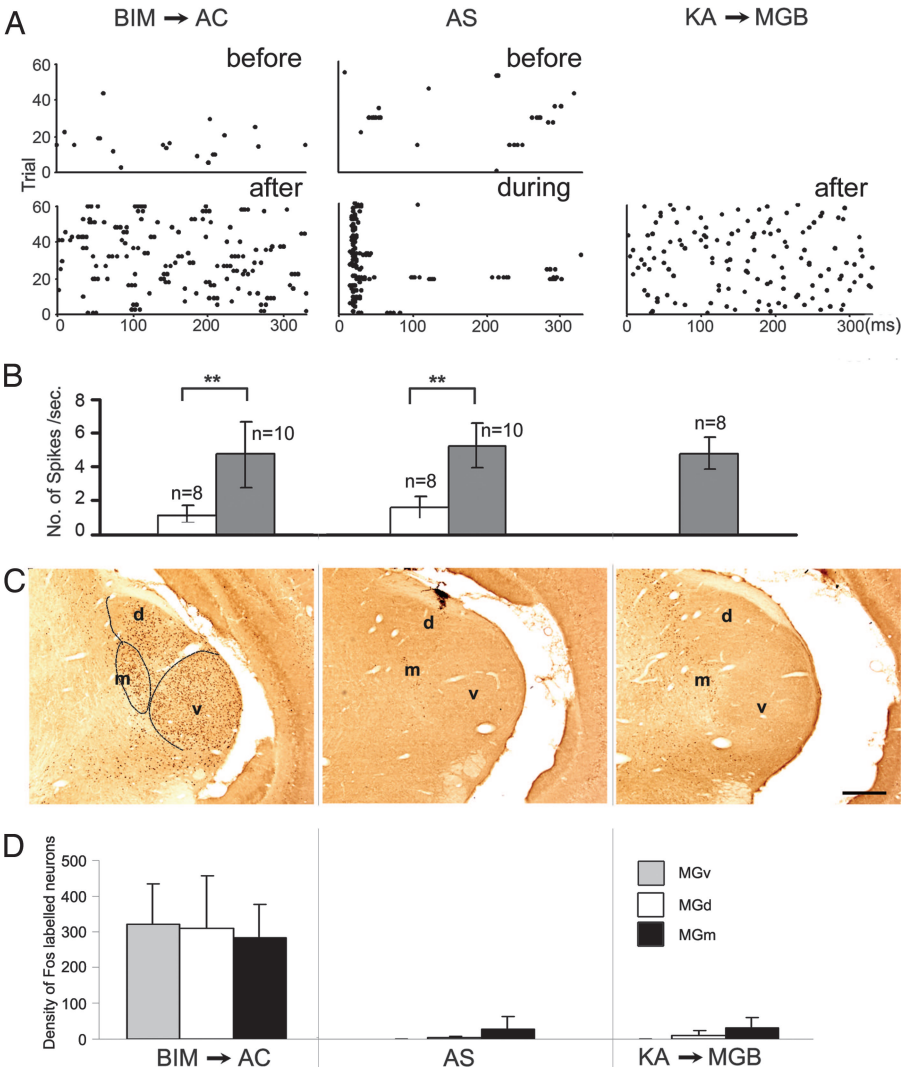

Fig. 4. Neuronal activities and *c-fos* expression in the MGB under three different conditions. (*A*) Raster displays show spontaneous firing before and after the BIM injection in the AC (BIM → ACx, *Left*), spontaneous firing and neuronal response to acoustic stimulus (AS, *Center*), and the spontaneous firing after KA injection into the MGB (KA → MGB, *Right*). Raster displays show spontaneous activities or auditory responses of neurons for 20 s (60 trials of 333 ms). (*B*) Bar chart showing the mean firing rate in different conditions as shown in *A*. Comparisons between the mean firing rates before and after BIM → AC and the mean firing rates before and during AS were significantly different (**, $P < 0.01$, *t* test). Comparison between the mean firing rates before BIM → AC and before AS and comparisons among the means of firing rates after BIM → AC, during AS, and after KA → MGB, were not significant (ANOVA, $P > 0.05$). (*C*) Photomicrographs showing *c-fos* expression of the three experimental paradigms. (*D*) Histogram showing the densities of Fos-positive neurons in the different divisions of MGB after BIM → AC ($n = 6$), after AS ($n = 3$), and after KA → MGB ($n = 2$). Significant differences ($P < 0.01$) were found among them. (Scale bar, 400 μm.)

Neuronal Activity and *c-fos* Expression. Generally, *c-fos* has been considered as a marker of neuronal activity or a marker of the increment of neuronal activity under certain conditions (14, 17, 20, 23). Although similar firing rates were observed in MGB neurons after (*i*) BIM injection to the AC, (*ii*) receiving a fast-repetitive acoustic stimulus, or (*iii*) direct KA injection to the MGB, only BIM injection to the AC produced dense *c-fos* expression in the MGB (Fig. 4).

KA is an excitotoxic agent that increases spontaneous neuronal activity within 2–4 h and damages neurons morphologically after 20 h (24). In the present study, Hyperactivity in the MGB was recorded after KA was injected into the MGB, and the rat was killed 1.5 h after injection. Although we could not exclude the possibility of neuronal damage by KA injection, the high firing rate of the MGB neurons gave evidence for their functionality.

It was necessary to activate the corticofugal pathway to induce *c-fos* expression in the MGv. Cortical activation caused synchronized burst firings in the MGB, suggesting that *c-fos* expression in the MGB may be linked to the burst firing pattern rather than the firing rate.

***c-fos* Expression in the Thalamus.** In animals exploring for a new environment, Montero and colleagues (25, 26) showed that *c-fos* expression in the TRN and LGN was elicited by the corticofugal pathway. The sensory thalamic nuclei received both ascending inputs from the brainstem and descending projections from the cortex and meanwhile were modulated by acetylcholine release from the brainstem or the basal forebrain (3). Corticothalamic terminals activate the thalamocortical neurons that expressed NMDA and non-NMDA ionotropic receptors as well as mGluR receptors (1, 27–31), whereas the ascending sensory terminals activated thalamocortical neurons that expressed only NMDA and AMPA ionotropic receptors (3, 32).

Direct injection of acetylcholine did not elicit *c-fos* expression, whereas glutamate elicited dense *c-fos* expression in the MGv (Fig. 1*C*). The present result proposes that *c-fos* expression in the MGv is related to the corticothalamic inputs mediated by AMPA, NMDA, and mGluR receptors. *c-fos* expression has been proposed to link with calcium influx, which then triggers a cascade of Ca^{2+}-sensitive gene expression (33–35). Extracellular Ca^{2+} influx can occur through various channels, such as NMDA receptors and L-type voltage-operated Ca^{2+} channels (36, 37). The mGluR1 receptor can also affect Ca^{2+} homeostasis and trigger Ca^{2+}-sensitive gene transcription in neurons. The present results show that all of the above three types of glutamate receptors are involved in *c-fos* expression.

Thalamocortical Oscillations and *c-fos* Expression. Neurons in the thalamus and cortex showed spontaneous activities even before the cortex was injected with BIM. The $GABA_A$ antagonist activated the auditory cortex. The interplay between the cortical and thalamic neurons (possibly including the TRN neurons) caused a rhythmic

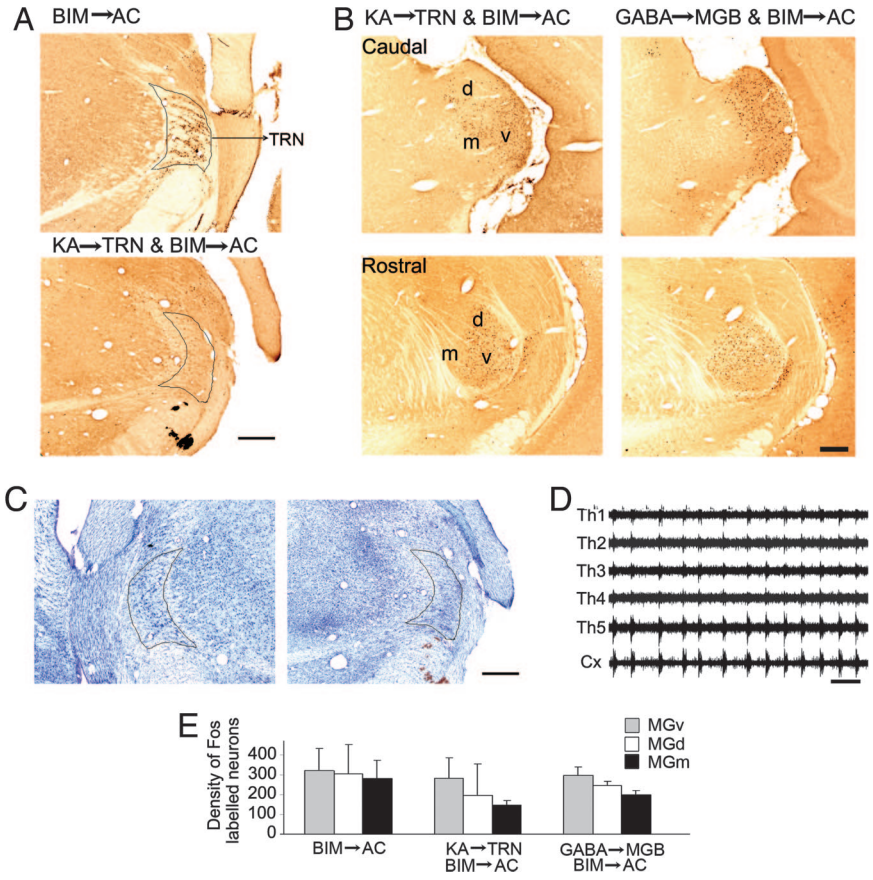

Fig. 5. Involvement of TRN. (*A*) Photomicrographs show *c-fos* expression in the auditory section of TRN. *c-fos* expression in the TRN was observed after BIM injection in the AC in rats with intact TRN (*Upper*). BIM injection in the AC did not result in *c-fos* expression in the TRN of rats with a selective lesion of TRN neurons by KA injection 2 days before the cortical BIM injection (*Lower*). (*B*) Photomicrographs show *c-fos* expressions in different coronal levels of the MGB after KA injection in the TRN and BIM injection in the AC (*Left*), and after GABA injection in the MGB, followed by BIM injection in the AC (*Right*). (*C*) Nissl staining showing the somas of the neurons in the left and right TRN after the right TRN was selectively destroyed with KA injection. (Scale bar, 400 μm.) (*D*) Spontaneous firings of multichannel recordings in the thalamus (Th1–5) and cortex (Cx) 10 min after BIM injection in the AC on the same preparation as illustrated in *B Left*. (Scale bar, 1 s). (*E*) Histogram showing densities of Fos-positive neurons in different divisions of MGB after BIM → AC ($n = 6$), TRN lesion group ($n = 3$), and GABA → MGB group ($n = 2$). No significant differences ($P > 0.05$) in the MGv and MGd were found among them.

oscillation at a frequency of 0.3–3 Hz. This oscillation gradually spread from the auditory cortex to the thalamus, resulting in a synchrony between them.

A striking finding is that the cortex started the oscillatory spontaneous activity before the thalamus (Fig. 3*A*). By suppressing the $GABA_A$ receptors after the injection of BIM into the cortex, the cerebral cortex would be excitotoxically activated, as shown in the *c-fos* expression in Fig. 1*B* (*Upper Right*). The hyperactivity of the cortex may activate the MGv directly via the projection neurons in layer VI of the auditory cortex (2, 12, 38). In contrast to the MGv, the contralateral auditory cortex showed no *c-fos* expression (Fig. 1*B Upper Left*). A very weak synchrony was detected in the electrodes that were implanted in the contralateral cortex (results not shown). This indicates that there is a much stronger interaction between the cortex and thalamus within the same hemisphere than that between the cortices of the two hemispheres.

The generation of the oscillation in the present study seemed not to depend on the TRN, because TRN inhibition only applied to the thalamus, and the cortex could develop the oscillation of similar rhythm before the thalamus. To address whether the thalamic oscillation was directly driven by corticothalamic projections or by the rebound from hyperpolarization derived from the TRN, we selectively destroyed the TRN neurons but not the fibers coursing through the TRN. We found that the MGB still showed the synchronized oscillation as that in the AC (Fig. 5*D*). Using a similar preparation, Timofeev *et al.* (39) concluded that thalamic neurons reflected cortical events as a function of the membrane potential in TRN/thalamocortical neurons and the degree of synchronization in cortical neuronal network. The present result indicates that the synchronized oscillation in the MGB could be generated without the participation of the TRN. In addition, the frequency and duration of the firing bursts in the thalamus did not change in TRN-lesioned animals. Our result from the *in vivo* preparation showing that thalamocortical oscillations could occur without the participation of the TRN is a great addition to our present understanding that most thalamocortical oscillations need the inhibitory interaction of the TRN neurons (8, 40–43).

In summary, *c-fos* expression in the MGB triggered by cortical activation was elicited via a direct corticothalamic pathway, not by the pathway through the TRN. *c-fos* expression in the MGB had a link to glutamate receptors (viz., NMDA, AMPA, and mGluR receptors) but not to acetylcholine receptors. The present results conclude that *c-fos* expression is not simply associated with firing rate, but rather the firing pattern. Burst firings of thalamic neurons synchronized with cortical oscillations are proposed to lead to *c-fos* expression in the MGB. The present results also imply that the corticothalamic projection is much stronger than the ascending collicular projection to the thalamus and is much stronger than the commissural projection between the two hemispheres.

Methods

Subjects. Sixty-four adult male Sprague–Dawley rats (220–380 g) were used for *c-fos* expression and extracellular recording experiments. The subjects were kept in the Laboratory Animal Unit at constant temperature (22°C) and on a regular 12-hour light/dark cycle. The experimental protocols were approved by the Animal Subjects Ethics SubCommittee of The Hong Kong Polytechnic University. See *SI Text* for detailed materials and methods.

Drug Applications. All drugs were bought from Sigma (St. Louis, MO) or Tocris (Bristol, UK), unless otherwise specified. Detailed procedures for animal preparation and injection of BIM in the AC have been described (19). Drug applications were made through a microinjection system (Hamilton, Reno, NV). Twenty-nine rats were injected with BIM alone in the AC, and saline (0.9% NaCl, 0.3 μl) was injected into the contralateral AC as a vehicle control.

Seven additional rats were injected in the MGB with either L-glutamate (L-Glu, 0.3 μl, 100 mM, pH 7–8, $n = 4$) or acetylcholine (Ach, 0.3 μl, 100 mM, pH 4.0, $n = 3$).

Nine rats were injected with one of three different glutamate receptor antagonists: AP-V (NMDA receptor antagonist, 100 mM, pH 8.0, $n = 3$), CNQX (AMPA receptor antagonist, 1 mM, pH 8.5, $n = 3$), and LY367385 (mGlu1α receptor antagonist, 0.5 mM, pH 7.4, $n = 3$). A total volume of 0.3 μl was consecutively injected four times at 20-min intervals in the MGB, starting before the AC was bilaterally activated with BIM and ending with sacrifice of animal. Saline (0.3 μl, 0.9% NaCl) was injected into the contralateral MGB as vehicle control in all animals. With the same injection strategy, GABA was injected into the MGB in two rats.

To directly activate the MGB neurons, two rats received KA (100 mM, 0.1 μl) injection into the MGB. To selectively lesion the TRN neurons, eight rats were injected with KA (100 mM, 0.3 μl) in the TRN at 2–7 days before BIM injection in the AC.

In all experiments, subjects survived for 1–1.5 h after BIM, Glu, Ach, or KA injections before they were killed. After sacrifice, Fos immunohistochemistry was performed.

Acoustic Stimuli and Extracellular Recording. Acoustic stimuli were generated digitally by a MALab system (Kaiser Instruments, Irvine, CA) (7, 44) or TDT auditory physiology workstation (Tucker-Davis Technologies, Alachua, FL). Seven rats were exposed only to repeated noise bursts or pure tones for 1–4 h under anesthesia without other manipulations before sacrifice and *c-fos* immunohistochemistry.

The EEG recorded in the contralateral cortical pericruciate area was used to monitor the anesthetic level of the subjects. Other procedures were the same as described (45). Two types of electrodes were used to record the cortical and thalamic neuronal activities: (*i*) an array of four or eight tungsten microelectrodes with a constant interelectrode distance of 0.5 mm and an impedance of 1–6 MΩ (FHC, Bowdoin, ME); (*ii*) a single tungsten microelectrode (impedance: 1–6 MΩ) attached to a glass micropipette (30–40 μm tip diameter) used for drug application. Penetrations were made according to the rat atlas, perpendicularly to the surface of the AC or vertically from the top of the brain to the MGB. Electrodes were advanced by using a stepping micromotor that was controlled outside the soundproof room. A preliminary mapping experiment was carried out to confirm the MGB and AC by acoustic responses. The recording electrode array was placed in the thalamus, with the central two/three electrodes targeting at the MGv (Fig. 3 *B* and *C*). The MGv neurons are characterized with short response latencies and easily defined characteristic frequency. The cortical electrodes were placed at a depth of 700–1,100 μm, targeting Layers V and VI of the primary AC. Spontaneous activities or acoustic responses of multiunits were simultaneously recorded in the MGB and AC, before, during, and after BIM injection into the AC.

Signals were A/D-converted (Axon Digital 1200) and filtered (300 Hz–5 kHz) before being stored in a computer for off-line analysis. Spikes of single-unit activity were detected with a home-made software window discriminator.

Histology. Parcellation of the MGB was based on the neural architecture of Nissl staining with reference to the published literature (46, 47). Histological processing for *c-fos* expression was performed as described (19, 48).

To examine the effectiveness of KA in selectively damaging TRN neurons, the TRN of rats with KA injection in the TRN were processed with Nissl staining.

Cell Counting and Statistical Analysis. Numerical results are expressed as means ± SD. Density (cells per unit area) of Fos-positive neurons was assessed. This measure allows the normalization of data in case different numbers of tissue sections were collected from different animals. A Student *t* test was used to examine the differences between two groups. ANOVA was used to examine the differences among three groups. The confidence level was taken at 95% ($P < 0.05$). Synchrony among different recording channels was quantified through cross-correlogram.

We thank Shigang He (Institute of Biophysics, Chinese Academy of Sciences) for critical comments and to Simon S. M. Chan and Kimmy F. L. Tsang (University of Hong Kong) for their excellent technical assistance. This work was supported by Hong Kong Research Grant PolyU 5467/05M.

1. Jones EG (1985) *The Thalamus* (Plenum, New York).
2. Ojima H (1994) *Cereb Cortex* 4:646–663.
3. Steriade M, Jones EG, McCormick DA (1997) *Thalamus* (Elsevier, Amsterdam).
4. Winer JA, Larue DT (1987) *J Comp Neurol* 257:282–315.
5. Murphy PC, Sillito AM (1987) *Nature* 329:727–729.
6. Villa AE, Rouiller EM, Simm GM, Zurita P, de Ribaupierre Y, de Ribaupierre F (1991) *Exp Brain Res* 86:506–517.
7. He JF (2003a) *J Neurophysiol* 89:367–381.
8. Steriade M, McCormick DA, Sejnowski TJ (1993) *Science* 262:679–685.
9. Bal T, Debay D, Destexhe A (2000) *J Neurosci* 20:7478–7488.
10. Golshani P, Jones EG (1999) *J Neurosci* 19:2865–2875.
11. Barth DS, MacDonald KD (1996) *Nature* 383:78–81.
12. He JF (2003b) *J Neurosci* 23:8281–8290.
13. Morgan JI, Cohen DR, Hempstead JL, Curran T (1987) *Science* 237:192–197.
14. Sagar SM, Sharp FR, Curran T (1989) *Science* 240:1328–1331.
15. Keilmann A, Herdegen T (1997) *Brain Res* 753:291–298.
16. Luo L, Ryan AF, Saint Marie RL (1999) *J Comp Neurol* 404:271–283.
17. Saint Marie RL, Luo L, Ryan AF (1999) *J Comp Neurol* 404:258–270.
18. Zhang JS, Kaltenbach JA, Wang J, Kim SA (2003) *Exp Brain Res* 153:655–660.
19. Sun X, Xia Q, Lai CH, Shum DKY, Chan Y-S, He JF (2007) *J Comp Neurol* 501:509–525.
20. Morgan IJ, Curran T (1991) *Annu Rev Neurosci* 14:421–451.
21. Xiong Y, Yu YQ, Chan Y-S, He JF (2004) *J Physiol (London)* 560:207–217.
22. Newton JR, Ellsworth C, Miyakawa T, Tonegawa S, Sur M (2004) *Nat Neurosci* 7:968–973.
23. Mouritsen H, Janssen-Bienhold U, Liedvogel M, Feenders G, Stalleicken J, Dirks P, Weiler R (2004) *Proc Natl Acad Sci USA* 101:14294–14299.
24. Lee SM, Friedberg MH, Ebner FF (1994) *J Neurophysiol* 71:1702–1715.
25. Montero VM (1997) *Neuroscience* 76:1069–1081.
26. Montero VM, Wright LS, Siegel F (2001) *Brain Res* 916:152–158.
27. Scharfman HE, Lu S-M, Guido W, Adams PR, Sherman SM (1990) *Proc Natl Acad Sci USA* 87:4548–4552.
28. McCormick DA, von Krosigk M (1992) *Proc Natl Acad Sci USA* 89:2774–2778.
29. Turner JP, Leresche N, Guyon A, Soltesz I, Crunelli V (1994) *J Physiol (London)* 480:281–295.
30. Tennigkeit F, Schwarz DWF, Puil E (1999) *J Neurophysiol* 82:718–729.
31. Golshani P, Warren RA, Jones EG (1998) *J Neurophysiol* 80:143–154.
32. Salt TE, Eaton SA (1996) *Prog Neurobiol* 48:55–72.
33. Lerea LS, Butler LS, McNamara JO (1992) *J Neurosci* 12:2973–2981.
34. Sheng M, McFadden G, Greenberg ME (1990) *Neuron* 4:571–582.
35. Jinnah HA, Egami K, Rao L, Shin M, Kasim S, Hess EJ (2003) *Dev Neurosci* 25:403–411.
36. Jahnsen H, Llinas R (1984) *J Physiol (London)* 349:227–247.
37. Tennigkeit F, Scharz DWF, Puil E (1998) *Neuroscience* 83:1063–1073.
38. Rouiller EM, Welker E (1991) *Hear Res* 56:179–190.
39. Timofeev I, Grenier F, Steriade M (1998) *J Neurophysiol* 80:1495–1513.
40. Guillery RW, Sherman SM (2002) *Neuron* 33:163–175.
41. Destexhe A, Bal T, McCormick DA, Sejnowski TJ (1996) *J Neurophysiol* 76:2049–2070.
42. McCormick DA, Bal T (1997) *Annu Rev Neurosci* 20:185–215.
43. Timofeev I, Grenier F, Bazhenov M, Houweling A, Sejnowski TJ, Stariade M (2002) *J Physiol* 542:583–598.
44. Semple MN, Kitzes LM (1993) *J Neurophysiol* 69:449–461.
45. He JF (2002) *J Neurophysiol* 88:2377–2386.
46. Redies H, Brandner S, Creutzfeldt OD (1989) *J Comp Neurol* 282:489–511.
47. He J (2001) *J Neurosci* 21:8672–8679.
48. Lai CH, Tse YC, Shum DK, Yung KK, Chan YS (2004) *J Comp Neurol* 470:282–296.